

# Enhanced normal scattering by lacunary gratings

G. Guida, D. Maystre, and G. Tayeb

*Laboratoire d'Optique Electromagnétique Unité de Recherche Associée au Centre National de la Recherche Scientifique No. 843, Faculté des Sciences et Techniques de St. Jérôme (Case 262), 13397 Marseille Cedex 20, France*

Received December 21, 1995; revised manuscript received September 18, 1996; accepted September 23, 1996

An intuitive presentation and a numerical verification are given of a phenomenon of enhanced normal scattering generated by lacunary gratings that are made by parallel rods. It is shown that the phenomenon can be explained by an interference between primary and multiscattered fields scattered by the cylinders when the distance between two arbitrary cylinders is a multiple of the wavelength. © 1997 Optical Society of America [S0740-3232(97)00203-2]

## 1. INTRODUCTION

In this paper we present a phenomenon of enhancement in normal direction of the scattered field generated by a lacunary grating, that is, a structure obtained from a finite periodic grid of  $N$  parallel cylinders by random removal of  $N_s$  cylinders.

It is well known that as a result of multiscattering, random structures such as randomly rough surfaces,<sup>1-5</sup> quasi-gratings,<sup>6</sup> and random sets of cylinders,<sup>7,8</sup> can generate enhanced backscattering phenomena. Since a lacunary grating can be considered a random structure (at least if the ratio  $N_s/N$  is not negligible), one can expect that such a structure could also generate the phenomenon of enhanced backscattering.

In fact, it has been observed<sup>8</sup> that in general, the peak of enhanced backscattering generated by a set of cylinders randomly located on a straight line remains small [especially for  $p$  polarization (TM)], because such a device weakens multiscattering phenomena. Indeed, it has been quite difficult for us to show, from our numerical computations, enhanced backscattering phenomena generated by lacunary gratings. On the other hand, when the period/wavelength ratio is close to an integer, a strong phenomenon of enhanced normal scattering can be found on theoretical scattering patterns. This phenomenon will be explained by an interference phenomenon in which the primary field scattered by each cylinder plays a role, in contrast to the current interpretation given to enhanced backscattering.

## 2. HEURISTIC PRESENTATION OF THE ENHANCED NORMAL-SCATTERING PHENOMENON

Figure 1 shows the current heuristic explanation of the enhanced backscattering phenomenon generated by a random set of cylinders. The two time-reversal pairs striking successively two arbitrary cylinders A and B interfere constructively in the backscattering direction (fields 1 and 2). For obvious reasons, the same constructive interference phenomenon holds in the symmetric di-

rection with respect to the plane of the cylinders (fields 3 and 4). In Fig. 2 we consider the interference between two fields:

- Field 1, the primary field scattered by cylinder A in the direction normal to the plane of cylinders A and B;
- Doubly scattered field 2 generated in the same direction by cylinder B and coming from A.

If the phase shift between the incident and the scattered fields of one cylinder is neglected, fields 1 and 2 are in phase if the distance AB is a multiple of the wavelength  $\lambda$ . Thus, in a lacunary grating deriving from a complete grating of period  $d = \lambda$ , the distance between two arbitrary cylinders is always a multiple of the wavelength, and one can conjecture a peak in the normal direction of scattering.

More generally, it is easy to find that the same constructive interference phenomenon holds in the directions of scattering orders generated by the grating illuminated in normal incidence. This property will be detailed in Subsection 4.G.

In contrast to the phenomenon of enhanced backscattering, the pair of emerging fields (1 and 2 for example) are not associated by a time-reversal process. In fact, it can be noticed that the number of emerging fields having the same phase is not limited to two, as shown in Fig. 2. Indeed, an incident field illuminating a cylinder A will generate a set  $\Sigma_A$  of doubly scattered fields in phase with the primary field 1. This set is composed of  $N - N_s - 1$  fields, since the field scattered by A illuminates all the other cylinders. Of course, the same reasoning applies to the multiscattered fields that have struck more than two cylinders (for instance, field 3 in Fig. 2). From this remark, it cannot be expected that the limitation to 100% of the enhancement observed in the backscattering direction remains valid for enhanced normal scattering.

On the other hand, the rules about the phase shift between two different sets  $\Sigma_A$  and  $\Sigma_{A'}$  remain similar to those given in the framework of the enhanced backscattering phenomenon. It increases with the incidence angle and the distance  $AA'$ . The consequence is that the

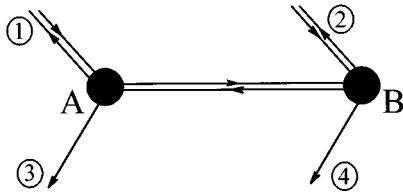


Fig. 1. Enhanced backscattering phenomenon: the two outgoing fields 1 and 2, deriving from fields diffracted by the two rods A and B, are in phase.

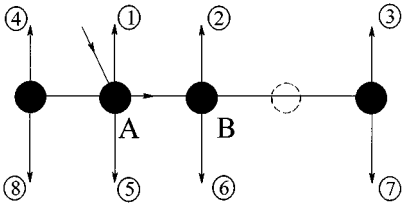


Fig. 2. For  $AB = n\lambda$  ( $n$  integer), outgoing fields 1, 2, 3, and 4 are in phase, as are 5, 6, 7, and 8.

normal scattering decreases when incidence angle increases, as shown in Subsection 4.C.

### 3. THEORIES

The lacunary grating is represented in Fig. 3. A monochromatic plane wave of wavelength  $\lambda = 2\pi/k$  illuminates the lacunary grating of  $N - N_s$  rods of index  $\nu$  ( $d$  denotes the period of the complete grating having  $N$  rods) that has incidence angle  $\alpha$  with respect to the  $y$  axis with counterclockwise convention. The angle of diffraction  $\theta$  is measured with respect to the  $x$  axis with the same convention.

The field scattered by a finite number of two-dimensional cylinders of arbitrary shape can be written, at infinity, in the form

$$E(P) = g(\theta) \frac{\exp(ikr)}{\sqrt{r}}, \quad (1)$$

where  $P$  is the point of observation in polar coordinates  $(r, \theta)$ , located at infinity ( $r \gg \lambda$ ). The intensity at infinity (or bistatic differential cross section) is defined by

$$D(\theta) = 2\pi|g(\theta)|^2. \quad (2)$$

So we have been able to calculate numerical data of  $g(\theta)$  and  $D(\theta)$  for lacunary gratings of arbitrary shape by using a recently developed computer code.<sup>8</sup> This code is based on a rigorous theory of scattering from a set of arbitrary-shaped parallel cylinders. In outline, the scattering matrices of each cylinder are calculated in an initial step, and then the scattering matrix of the entire set of cylinders is deduced from all these elementary scattering matrices by inverting a complex matrix. Numerous numerical tests (convergence, energy balance, reciprocity, and comparison with other codes) have shown that the numerical error tends to zero when the size of the matrix is increased. The reader can consider that the relative accuracy of our numerical results is better than 1% throughout this paper.

Since our intuitive prediction of the phenomenon of enhanced normal scattering relies on an interference between primary and multiscattered fields scattered by cylinders, we thought it would be interesting to compare our rigorous results with approximate results carried out with neglect of the multiscattering phenomena. The scattering pattern deduced from this approximate theory will be used to detect, in the rigorous results, the contribution of multiscattering.

Let us call  $g_o(\theta)$  the amplitude scattered at infinity by one cylinder placed at the origin of the coordinates system. Assuming that the field scattered by each cylinder is not modified by the other cylinders of the lacunary grating, straightforward calculations show that the field scattered at infinity by the lacunary grating can be approximated by

$$\tilde{g}(\theta) = g_o(\theta) \left[ \exp[i(N - 1)\phi/2] \frac{\sin(N\phi/2)}{\sin(\phi/2)} - \sum_{\substack{n \in [1, N] \\ n \notin \mathcal{N}}} \exp(i(n - 1)\phi) \right], \quad (3)$$

with

$$\phi = kd(\sin \alpha - \cos \theta), \quad (4)$$

and  $\mathcal{N}$  denotes the set of the remaining cylinders.

In order to check our heuristic interpretation of enhanced normal scattering, we thought it would be interesting also to include calculations that take into account primary and doubly scattered fields only (see Subsection 4.B, Fig. 8). For the sake of simplicity, this approximation will not be described in the present paper. The interested reader can refer to a recent paper<sup>9</sup> for details.

In outline, three theories will be used in the following: the rigorous theory, which provides a full description of multiscattering phenomena, and two approximate theories, the simplest one neglecting multiscattering and the second one taking into account primary and doubly scattered fields.

### 4. RESULTS

In this section we consider the mean intensities  $\langle D(\theta) \rangle$ , obtained by averaging the intensities  $D_q(\theta)$  ( $q \in [1, Q]$ ) scattered at infinity by a large number  $Q$  of random realizations of lacunary gratings.

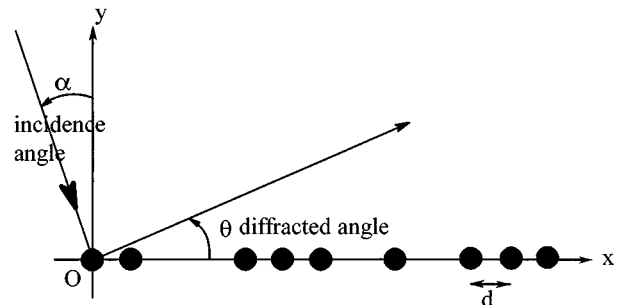


Fig. 3. Notation.

### A. Phenomenon of Enhanced Backscattering

To get the best conditions for enhanced backscattering, we chose the parameters of the cylinders so as to minimize the backscattered primary field. Figure 4 shows

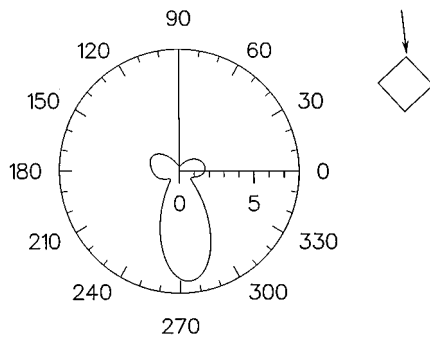


Fig. 4. Intensity of the field scattered at infinity by a single perfectly conducting rod placed at the origin. Its shape is square (one side is  $a = 0.7\lambda$ ) and rotated  $45^\circ$  with respect to the  $z$  axis. The rod is illuminated by an  $s$ -polarized (TE) plane wave with an incidence  $\alpha = 5^\circ$  with respect to the normal direction of the grating.

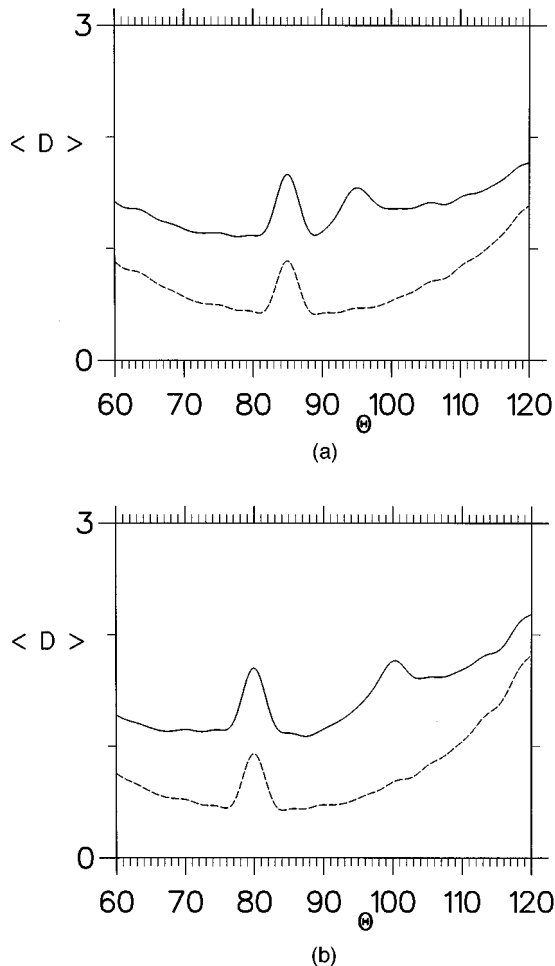


Fig. 5. Average of  $D(\theta)$  over 1,000 random realizations of lacunary gratings having two rods ( $d = \lambda$ ,  $N = 15$  and  $N_s = 13$ ) identical to the rod of Fig. 4. The incidence is (a)  $\alpha = 5^\circ$  (the backscattering direction is  $95^\circ$ ), (b)  $\alpha = 10^\circ$  (the backscattering direction is  $100^\circ$ ). Dashed curve, average of  $D(\theta)$  computed with neglect of multiscattering.

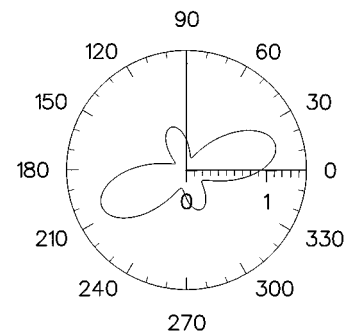


Fig. 6. Intensity of the field scattered at infinity by a single dielectric circular rod placed at the origin, with radius  $a = 0.22\lambda$  and index  $\nu = 3.2$ . The rod is illuminated by a  $p$ -polarized (TM) plane wave with incidence  $\alpha = 20^\circ$ .

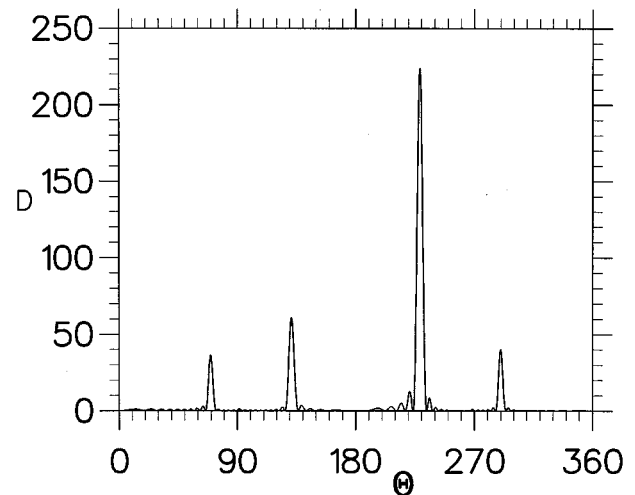


Fig. 7. Intensity of the field scattered at infinity for a finite grating of 15 circular rods ( $N = 15$ ) of radius  $a = 0.22\lambda$  and index  $\nu = 3.2$ . The grating is illuminated by a  $p$ -polarized (TM) plane wave with incidence  $\alpha = 20^\circ$  and period  $d = \lambda$ .

the scattering pattern of a perfectly conducting square rod (see square on the right-hand side of Fig. 4) illuminated by an  $s$ -polarized (TE) plane wave of wavelength  $\lambda$ . Figure 5(a) shows the scattering pattern of a lacunary grating of period  $d = \lambda$  with  $N = 15$  and  $N_s = 13$  (lacunary defect ratio  $N_s/N = 0.867$ ) illuminated by an  $s$ -polarized (TE) plane wave with the same angle of incidence  $\alpha = 5^\circ$ . Even though it seems strange to classify as a lacunary grating such a structure (it contains only two rods!) it must be confessed that it is the only one for which we have been able to find a weak phenomenon of enhanced backscattering. Here the peak of enhanced backscattering is located at  $\theta = \alpha + 90^\circ = 95^\circ$ , the peak at  $\theta = -\alpha + 90^\circ = 85^\circ$  corresponding to the specularly reflected field. Figure 5(b) corresponds to an angle of incidence of  $10^\circ$  and shows that the peak of enhanced backscattering follows the angle of incidence. The dashed curves show that the enhanced backscattering phenomenon vanishes when the multiscattering effect is neglected.

### B. Numerical Evidence of the Phenomenon of Enhanced Normal Scattering

According to Fig. 2, the phenomenon of enhanced normal scattering requires a good intensity both in the normal di-

rection ( $\theta = 90^\circ$  or  $270^\circ$ ) and in the orthogonal direction ( $\theta = 0^\circ$  or  $180^\circ$ ). Figure 6 shows the scattering pattern of a dielectric cylinder illuminated by a *p*-polarized (TM) plane wave. Obviously, this rod satisfies the required conditions. In Figure 7 the scattering pattern of a com-

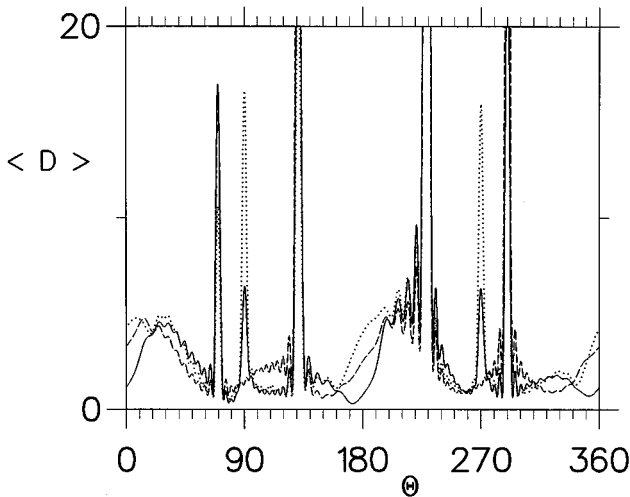


Fig. 8. Solid curve, average of  $D(\theta)$  over 1,000 realizations of lacunary gratings having 10 rods ( $N = 15$ ,  $N_s = 5$ ) starting from the complete grating of Fig. 7. Lacunary gratings are illuminated by a *p*-polarized (TM) plane wave with incidence  $\alpha = 20^\circ$ . Dashed line curve, same as solid curve but computed with neglect of multiscattering. Dotted curve, the same but computed by taking into account single and double scattering only.

plete grating with period  $d = \lambda$  and  $N = 15$  with incidence angle  $\alpha = 20^\circ$  is given. Two reflected and two transmitted (0 and  $-1$ ) orders exist. Figure 8 shows the same result but for a lacunary grating with a lacunary defect ratio equal to  $1/3$ . The peaks of enhanced normal scattering are located at  $\theta = 90^\circ$  (in reflection) and  $\theta = 270^\circ$  (in transmission). It is worth noticing that the height of the peak in the normal direction of reflection reaches almost 40% of that corresponding to the zeroth reflected order ( $\theta = 70^\circ$ ). Obviously, the enhancement exceeds 100%, as conjectured in Section 2. The figure clearly shows that multiscattered fields have a vital importance in the phenomenon. The dotted curve shows that the phenomenon exists when primary and doubly scattered fields only are taken into account. However, a quantitative description requires the use of higher orders of scattering.

**C. Influence of the Angle of Incidence**

Figure 9 shows the scattering patterns obtained by varying the angle of incidence, starting from the parameters of Fig. 8. It clearly appears that the height of the peak decreases when the angle of incidence is increased. In practice, the peak disappears at  $\theta = 50^\circ$ . This evolution can be explained in the same way as the decrease of enhanced backscattering with the angle of incidence (coherence of the interference phenomena between the two extremities of the grating) but also by Fig. 6: indeed, the cylinder has been chosen so as to favor the phenomenon in the vicinity of normal incidence.

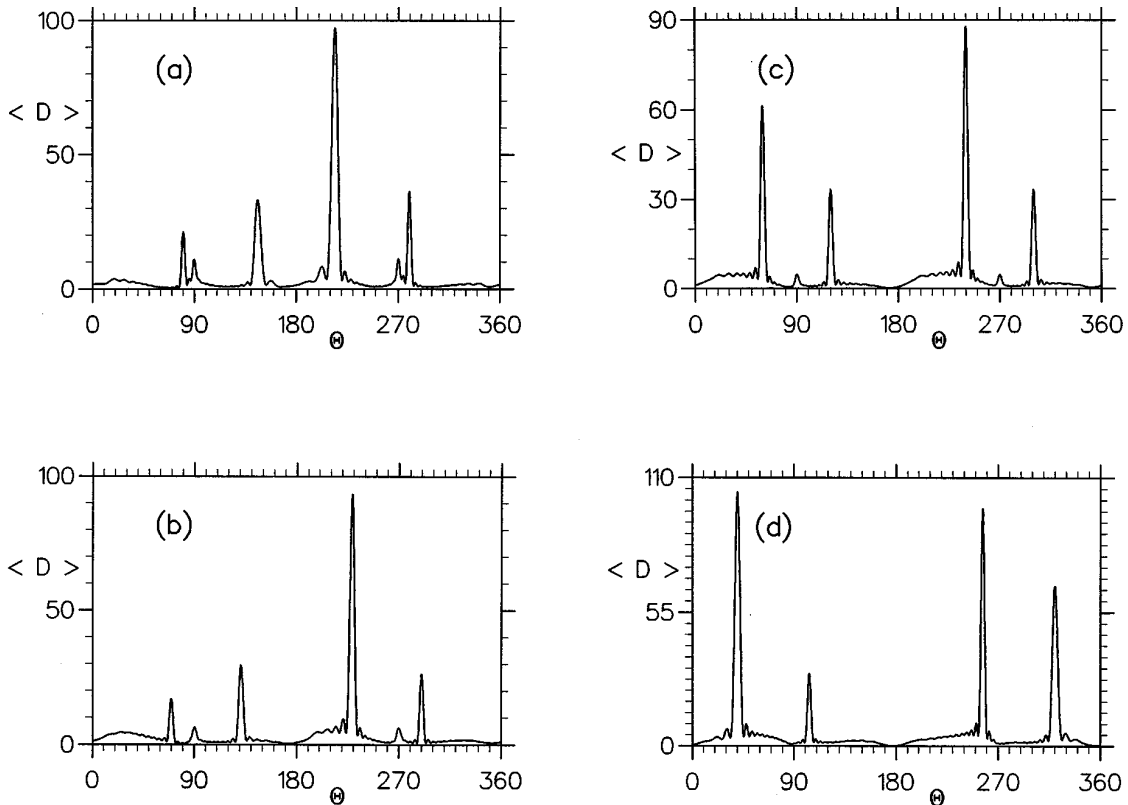


Fig. 9. Influence of the angle of incidence on the enhanced normal-scattering phenomenon: same parameters as Fig. 8 except that (a)  $\alpha = 10^\circ$ , (b)  $\alpha = 20^\circ$ , (c)  $\alpha = 30^\circ$ , and (d)  $\alpha = 50^\circ$ .

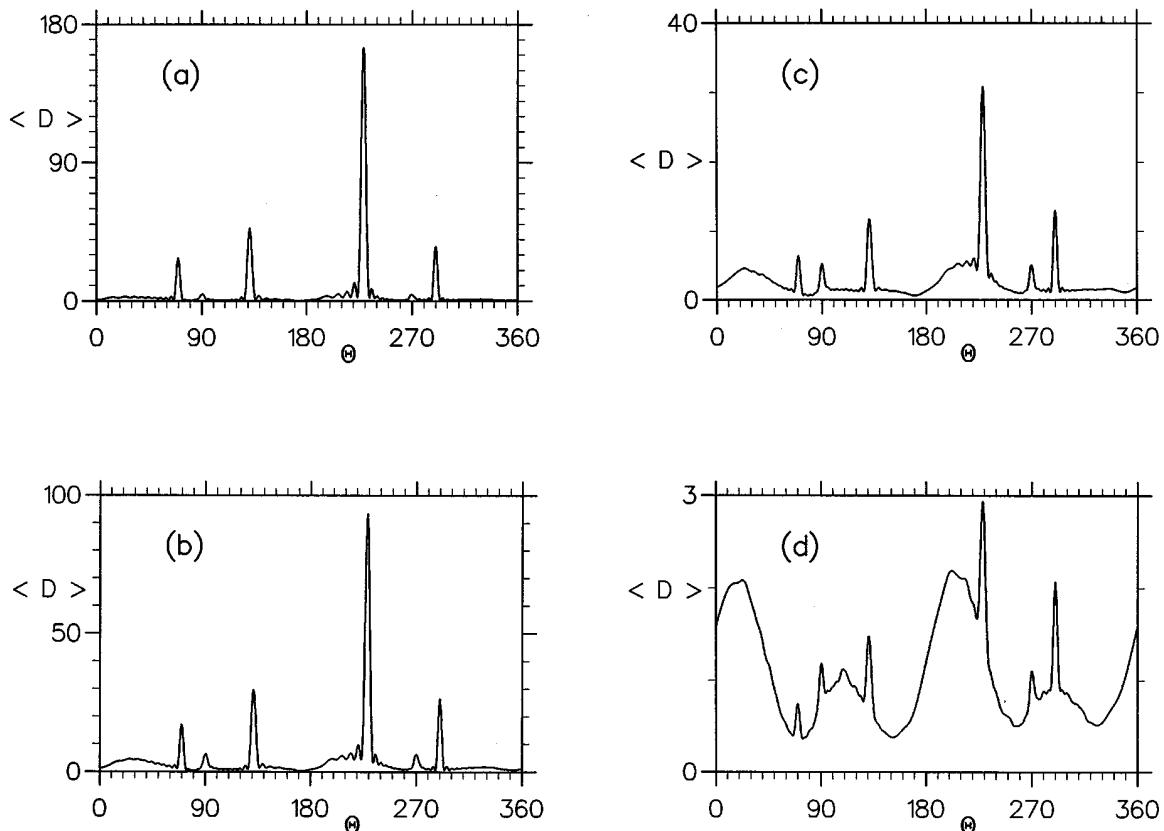


Fig. 10. Influence of the lacunary defect ratio: same parameters as Fig. 8 except for the number of remaining rods in the lacunary gratings: (a) 13 rods ( $N_s = 2$ ), (b) 10 rods ( $N_s = 5$ ), (c) 6 rods ( $N_s = 9$ ), and (d) 2 rods ( $N_s = 13$ ).

#### D. Influence of the Lacunary Defect Ratio

Figure 10 is obtained by varying  $N_s$  from Fig. 8. Peaks of enhanced normal scattering always appear. Note that the largest peaks over background ratios are obtained for the smallest values of the lacunary defect ratios. It is noteworthy that in Fig. 10(d) the lacunary grating contains two cylinders only. However, the phenomenon of enhanced normal scattering still holds, since the distance between the two scatterers is a multiple of the wavelength.

#### E. Influence of $N$ When the Lacunary Defect Ratio Is Kept Constant

Figure 11 shows the variation of the enhanced normal-scattering peak when the initial number of rods is increased, the lacunary defect ratio being kept constant. It turns out that broadly speaking, the height of the peak is proportional to  $N$ , whereas its width decreases as  $1/N$ . From numerous other calculations, we deduced that the width of the enhanced normal-scattering peak is the same as the width of the grating orders and depends on the grating size over the wavelength ratio only.

#### F. Influence of the $d/\lambda$ Ratio

So far, we have dealt with a period of the lacunary grating equal to the wavelength  $\lambda$ , i.e., in the actual condition given in the heuristic explanation. Figure 12 shows the scattering pattern obtained in the vicinity of  $270^\circ$  for a lacunary grating with  $\alpha = 10^\circ$ ,  $N = 15$ ,  $N_s = 9$ ,  $\nu = 3.2$ ,

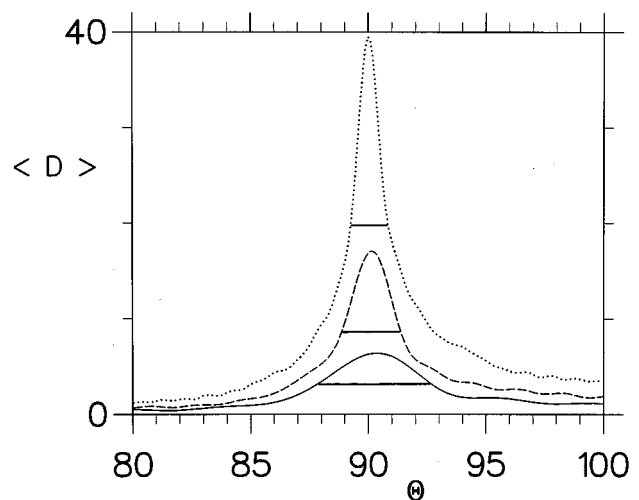


Fig. 11. Influence of  $N$  when the lacunary defect ratio is kept constant and equal to  $1/3$ . Same parameters as in Fig. 8. Solid curve,  $N = 15$ ; dashed line curve,  $N = 30$ ; dotted line curve,  $N = 60$ .

and  $a = 0.22\lambda$ , successively with  $d = \lambda$  (solid curve) and  $d = 1.05\lambda$  (dashed curve). When  $d$  differs slightly from  $\lambda$ , the peak in the normal direction of diffraction is split into a couple of peaks. Figure 13(a) gives the intuitive explanation of this split: owing to the increase in the optical path between A and B, the primary field 1 scattered by A and the secondary field 2 scattered by B are in phase

in a direction of diffraction slightly different from  $\theta = 90^\circ$ . A straightforward calculation shows that the shift of the diffraction angle is equal to  $\sin^{-1}[\epsilon/(n\lambda + \epsilon)] \approx 3^\circ$ . The peak in the symmetrical direction with respect to the normal is depicted in Fig. 13(b). It is due to the interference between the primary field scattered by B and the secondary field scattered by A.

**G. Enhanced Scattering in the Direction of the Orders Generated by the Grating Illuminated in Normal Incidence**

Let us show that the enhancement of the scattered field may occur not only in the normal direction but also in some other directions that can be easily predicted from the grating formula. Figure 14 represents the scattering

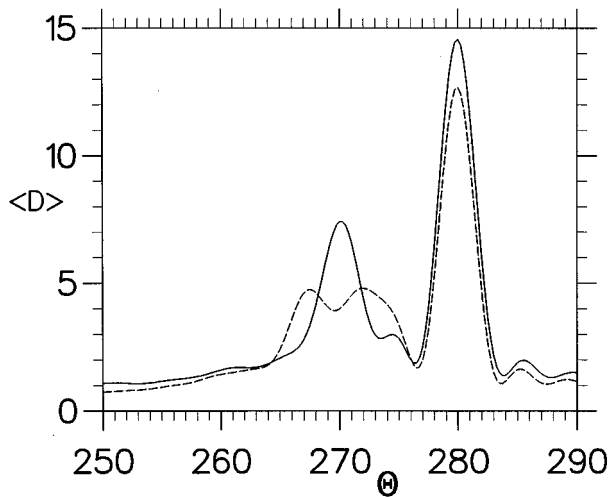


Fig. 12. Average of  $D(\theta)$  over 1,000 realizations of lacunary gratings having six circular rods ( $N = 15$  and  $N_s = 9$ ) of index  $\nu = 3.2$  and radius  $a = 0.22 \lambda$ , for a period of the initial complete grating  $d = \lambda$  (solid curve) and  $d = 1.05 \lambda$  (dashed curve). Lacunary gratings are illuminated by a  $p$ -polarized (TM) plane wave with incidence  $\alpha = 10^\circ$ .

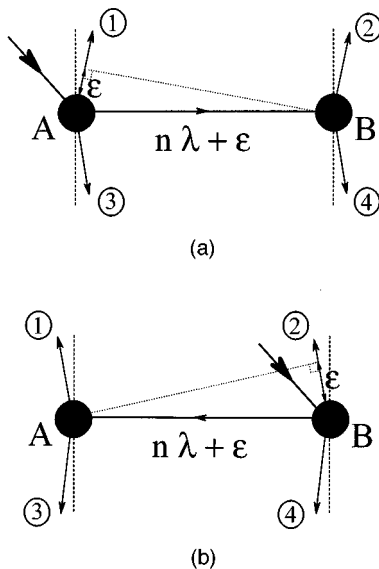


Fig. 13. Split of peaks: outgoing fields 1 and 2 are in phase, as are 3 and 4.

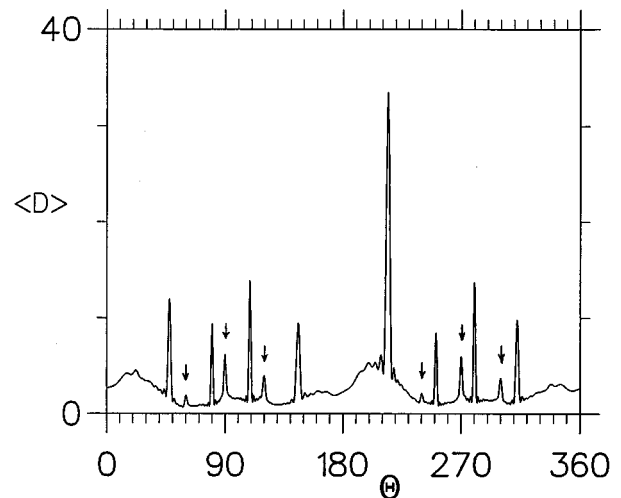


Fig. 14. Average of  $D(\theta)$  over 1,000 realizations of lacunary gratings having six circular rods ( $N = 15$  and  $N_s = 9$ ) of index  $\nu = 3.2$ , radius  $a = 0.22 \lambda$  and period of the initial complete grating  $d = 2 \lambda$ . Lacunary gratings are illuminated by a  $p$ -polarized (TM) plane wave with incidence  $\alpha = 10^\circ$ .

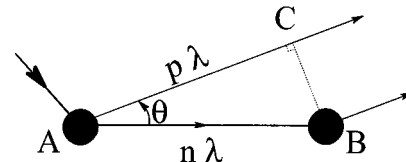


Fig. 15. Enhanced scattering in the directions of the orders generated by the grating illuminated at normal incidence.

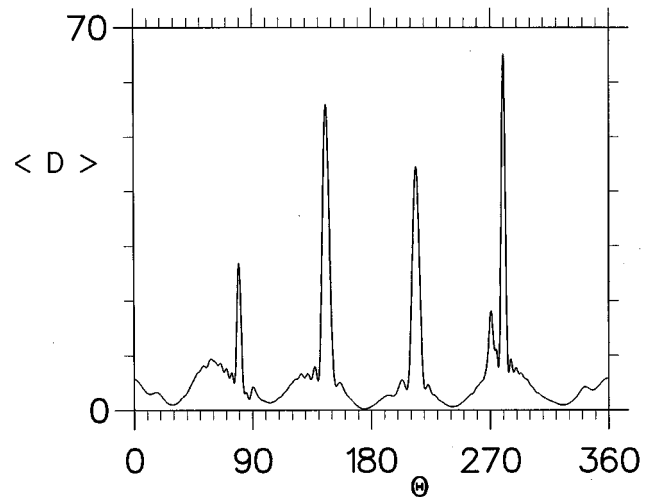


Fig. 16. Enhanced normal scattering for the  $s$ -polarization case (TE): average of  $D(\theta)$  over 1,000 random realizations of lacunary gratings having six circular rods ( $N = 15$  and  $N_s = 9$ ) of radius  $a = 0.41 \lambda$  and index  $\nu = 2.3$ . Gratings are illuminated by an  $s$ -polarized (TE) plane wave with incidence angle  $\alpha = 10^\circ$  and period of the initial complete grating  $d = \lambda$ .

pattern obtained for a lacunary grating with  $d = 2\lambda$  and  $\alpha = 10^\circ$ . The highest eight peaks correspond to the directions of the orders of the grating of period  $2\lambda$  illuminated at  $10^\circ$  of incidence (peaks without arrows). Six other peaks appear at  $\theta = 60^\circ, 90^\circ, 120^\circ, 240^\circ, 270^\circ$ , and  $300^\circ$ . Once more, a simple heuristic explanation can be

given. In Fig. 15, one can see that the primary field scattered by A and the secondary field scattered by B are in phase, provided that  $AB = n\lambda$  and  $AC = p\lambda$  ( $n$  and  $p$  integers). Obviously, the value  $p = 0$  corresponds to the enhanced normal scattering in the directions  $\theta = 90^\circ$  and  $\theta = 270^\circ$ . More generally, it is easy to verify that the different values of  $p$  give directions of enhanced scattering that correspond to the orders of a grating of period  $d = n\lambda$  but illuminated in normal incidence.

#### H. Example in s-Polarization (TE)

Figure 16 shows the scattering pattern of a dielectric lacunary grating with circular rods. The enhancement in the normal directions of scattering is close to 100%. Thus, as can be conjectured from our heuristic explanation, polarization seems not to play a fundamental role in the phenomenon.

## 5. CONCLUSION

A phenomenon of enhanced normal scattering generated by lacunary gratings has been described and explained intuitively. For this kind of structure this phenomenon is much greater than the classical phenomenon of enhanced backscattering. Obviously, the same phenomenon should occur for lacunary relief gratings (for example, lacunary lamellar gratings) or even three-dimensional lacunary gratings (deduced from a grating made with spheres). In the same way, a strong phenomenon of enhanced normal scattering should be obtained by illuminating a quasi-crystal with two rhombs having sides equal to a multiple of the wavelength.

## ACKNOWLEDGMENT

The work described in this paper was done under a contract between the Laboratoire d'Optique Electromagnétique and the Direction des Recherches Etudes et Techniques (French ministry of Defense).

## REFERENCES

1. A. Ishimaru, J. S. Chen, P. Phu, and K. Yoshitomi, "Numerical, analytical, and experimental studies of scattering from very rough surfaces and backscattering enhancement," presented at the International Workshop on Modern Analysis of Scattering Phenomena, Aix en Provence, France, September 5–8, 1990.
2. M. J. Kim, J. C. Dainty, A. T. Friberg, and A. J. Sant, "Experimental study of enhanced backscattering from one- and two-dimensional random rough surfaces," *J. Opt. Soc. Am. A* **7**, 569–577 (1990).
3. V. Celli, A. A. Maradudin, A. M. Marvin, and A. R. McGurn, "Some aspects of light scattering from a randomly rough metal surface," *J. Opt. Soc. Am. A* **2**, 2225–2239 (1985).
4. J. M. Soto-Crespo and M. Nieto-Vesperinas, "Electromagnetic scattering from very rough random surfaces and deep reflection gratings," *J. Opt. Soc. Am. A* **6**, 367–384 (1989).
5. K. A. O'Donnell and E. R. Mendez, "Experimental study of scattering from characterized random surfaces," *J. Opt. Soc. Am. A* **4**, 1194–1205 (1987).
6. D. Maystre and M. Saillard, "Enhanced backscattering and blazing effect from gratings, quasi-gratings and randomly rough surfaces," *Waves Random Media* **4**, 467–485 (1994).
7. J. J. Greffet, "Backscattering of s-polarized light from a cloud of small particles above a dielectric substrate," *Waves Random Media* **3**, S65–S73 (1991).
8. D. Felbacq, G. Tayeb, and D. Maystre, "Scattering by a random set of parallel cylinders," *J. Opt. Soc. Am. A* **11**, 2526–2538 (1994).
9. G. Guida, G. Tayeb, and D. Maystre, "Scattering by lacunary gratings," *J. Mod. Opt.* (to be published).